



The High Molecular Gas Content, and the Efficient Conversion of Neutral into Molecular Gas, in Jellyfish Galaxies

Alessia Moretti¹ , Rosita Paladino² , Bianca M. Poggianti¹ , Paolo Serra³ , Mpati Ramatsoku^{3,4,5} , Andrea Franchetto^{1,6} , Tirna Deb⁷, Marco Gullieuszik¹ , Neven Tomičić¹ , Matilde Mingozzi¹ , Benedetta Vulcani¹ , Mario Radovich¹ ,

Daniela Bettoni¹ , and Jacopo Fritz⁸

¹ INAF-Padova Astronomical Observatory, Vicolo dell'Osservatorio 5, I-35122 Padova, Italy; alessia.moretti@inaf.it

² INAF-Istituto di Radioastronomia, via P. Gobetti 101, I-40129 Bologna, Italy

³ INAF-Cagliari Astronomical Observatory, Via della Scienza 5, I-09047 Selargius (CA), Italy

⁴ Department of Physics and Electronics, Rhodes University, P.O. Box 94, Makhanda, 6140, South Africa

⁵ South African Radio Astronomy Observatory, 2 Fir Street, Black River Park, Observatory, Cape Town, 7405, South Africa

⁶ Dipartimento di Fisica e Astronomia "Galileo Galilei," Università di Padova, vicolo dell'Osservatorio 3, I-35122 Padova, Italy

⁷ Kapteyn Astronomical Institute, University of Groningen, Postbus 800, NL-9700 AV Groningen, The Netherlands

⁸ Instituto de Radioastronomía y Astrofísica, UNAM, Campus Morelia, AP 3-72, CP 58089, Mexico

Received 2020 May 23; revised 2020 June 22; accepted 2020 June 23; published 2020 July 10

Abstract

In the disks of four jellyfish galaxies from the GASP sample at redshift ~ 0.05 we detect molecular gas masses systematically higher than in field galaxies. These galaxies are being stripped of their gas by ram pressure from the intracluster medium and are, in general, forming stars at a high rate with respect to nonstripped galaxies of similar stellar masses. We find that, unless giant molecular clouds in the disk are unbound by ram pressure leading to exceptionally high CO-to-H₂ conversion factors, these galaxies have a molecular gas content 4–5 times higher than normal galaxies of similar masses, and molecular gas depletion times ranging from ~ 1 to 9 Gyr, corresponding to generally very low star formation efficiencies. The molecular gas mass within the disk is a factor between 4 and ~ 100 times higher than the neutral gas mass, as opposed to the disks of normal spirals that contain similar amounts of molecular and neutral gas. Intriguingly, the molecular plus neutral total amount of gas is similar to that in normal spiral galaxies of similar stellar mass. These results strongly suggest that ram pressure in disks of galaxies during the jellyfish phase leads to a very efficient conversion of HI into H₂.

Unified Astronomy Thesaurus concepts: [Disk galaxies \(391\)](#); [Galaxy clusters \(584\)](#); [Molecular gas \(1073\)](#)

1. Introduction

What ultimately regulates galaxy evolution is the availability of gas prone to star formation, and its efficiency in forming new stars (Schmidt 1959; Kennicutt 1998). Therefore, in the last years, a lot of effort has been dedicated to building statistically significant samples of galaxies with observational coverage able to map all the gas phases, with the aim of discovering the underlying scaling relations that correlate the neutral and molecular gas content with the stellar mass, if any (Cortese et al. 2011; Saintonge et al. 2011a, 2011b; Corbelli et al. 2012; Catinella et al. 2018). More recent results also include the dust contribution (Casasola et al. 2020).

Scaling relations have been derived, in fact, for the HI content of nearby galaxies (Bigiel et al. 2008, 2010) while only small samples exist at higher redshifts (Fernández et al. 2016; Cortese et al. 2017; Catinella et al. 2018), suggesting that the gas in the molecular phase was the predominant fraction at early epochs.

As for the cold gas content, the largest statistical sample for which a homogeneous set of data has been collected so far is the COLDGASS (Saintonge et al. 2011a) sample together with its low mass extension xCOLDGASS (Saintonge et al. 2017). Galaxies in the xCOLDGASS sample are mass-selected at $z = 0.01$ – 0.05 , without any a priori bias on the IR/UV fluxes, and cover a range in stellar mass between 10^9 and $10^{11.5} M_{\odot}$. While this sample gives a wonderful insight into the gas properties of galaxies in general, it has not been designed to cover galaxies in different environmental conditions, i.e., it does not distinguish between galaxy properties in clusters and

those in the field, which are expected to behave differently. While early works on the Virgo and Coma clusters (Kenney & Young 1989; Boselli et al. 1997) have revealed no significant molecular gas deficiency in cluster galaxies (including the most HI deficient), more recent studies that make use of larger samples and better resolution find, instead, that HI gas stripped galaxies also have a lower H₂ content, albeit in lower proportion (Boselli et al. 2014). Similar results are also given by Corbelli et al. (2012), who study 35 metal-rich spiral galaxies that are part of the Herschel Virgo Cluster Survey. These galaxies have a well determined HI deficiency parameter, which has been found to anticorrelate with the molecular gas fraction, i.e., the ratio between molecular gas mass and stellar mass. Indeed, the molecular gas fraction has been found to decrease as the HI deficiency increases, while the ratio between the molecular and the total gas increases. This has been interpreted as due to the fact that both neutral and molecular gas are stripped, but the former is stripped more easily than the latter.

Single dish and, more recently, interferometric ALMA data have confirmed a normal molecular gas content in the disk of ESO137-001, a jellyfish galaxy in the nearby Norma cluster (Jáchym et al. 2014, 2019), albeit confined in a very small central region (with ~ 1.5 kpc radius), with a similar amount of molecular gas detected along the stripped tail. The D100 galaxy close to the Coma cluster center, instead, shows a higher than expected molecular gas fraction within the central ~ 2 kpc radius (Jachym et al. 2017), and a very H₂ rich gas tail, as traced by the CO emission.

A clear view on the molecular gas content of cluster galaxies subject to ram-pressure stripping is still missing, and we can now start to cast light on the subject by using the multi-wavelength data set collected by the GASP sample. The GASP survey⁹ (Poggianti et al. 2017b) has started exploring the effects of environmental interactions on nearby ($z \sim 0.05$) cluster/group galaxies thanks to a dedicated VLT MUSE Large Program (GAs Stripping Phenomena in galaxies with MUSE, P. I. B. Poggianti) mainly tracing the ionized gas, but complementary data sets at different wavelengths are being collected and have started offering a clear view on all the connected gas phases (see also George et al. 2018; Poggianti et al. 2019; Ramatsoku et al. 2019, 2020; Deb et al. 2020). In particular, in Moretti et al. (2018) we observed with the APEX telescope 4 GASP galaxies detecting molecular gas both in the galaxy disks and in the ionized gas tails.

We then started an observational campaign devoted to measuring the molecular gas content of these galaxies using ALMA interferometric data at ~ 1 kpc resolution. We have described the observations and the data analysis in Moretti et al. (2020), where we have shown the results for the JW100 galaxy. Surprisingly, in this galaxy we have found an anomalously large content of molecular gas, even excluding the new molecular gas possibly born in the tail from the stripped neutral gas. Assuming the standard conversion factor, we tentatively concluded that the star formation efficiency (SFE), i.e., the star formation rate (SFR) surface density divided by the H_2 mass density, on scales of 1 kpc shows a gradient moving from the central part of the disk toward the stripped tail, and the corresponding depletion time is always longer than the typical τ_{dep} of nearby disk galaxies (i.e., ~ 1 –2 Gyr, Bigiel et al. 2011; Leroy et al. 2013), increasing from the disk to the tail.

In this paper we analyze the ALMA Band 3 data of the four GASP galaxies observed in cycle 5 to understand whether their molecular gas content is following the scaling relations of normal galaxies, or if instead they are depleted/enriched, in molecular gas.

All the GASP galaxies here analyzed are operatively defined as jellyfishes (as they possess ionized gas tails whose length is comparable to the galaxy disk diameter, Poggianti et al. 2017a), and they also have a central AGN. Stellar masses and redshifts are given in Moretti et al. (2018), while results from MUSE data are described in Poggianti et al. (2017b), Bellhouse et al. (2017), Gullieuszik et al. (2017), Poggianti et al. (2019), and Moretti et al. (2020).

Throughout this paper we will make use of the standard cosmology $H_0 = 70 \text{ km s}^{-1} \text{ Mpc}^{-1}$, $\Omega_M = 0.3$, and $\Omega_\Lambda = 0.7$. As in the other GASP papers, our stellar masses are calculated adopting a Chabrier (2003) initial mass function (IMF).

2. Data and Analysis

Observations of the CO(1–0) emission (rest frequency 115.271 GHz) of our four galaxies, namely JO201, JO204, JO206, and JW100, have been obtained with ALMA during Cycle 5 (project 2017.1.00496.S). The spectral configuration used yields a velocity resolution of 3.1 km s^{-1} , which has been smoothed to 20 km s^{-1} in the final data cubes used for the following analysis. In order to cover with homogeneous sensitivity the entire area observed with MUSE, including disk

Table 1

Properties of CO(1–0) Line Images: Observed Frequency, Synthesized Beam (θ_{maj} , θ_{min} , and PA), rms, and Maximum Recoverable Scale (MRS; Equation (7) in the ALMA Technical Handbook)

Galaxy	ν_{obs} GHz	θ_{maj} "	θ_{min} "	PA deg	rms mJy b^{-1}	MRS "
JO201	110.307	1.99	1.57	−84.6	0.5	20
JO204	110.625	1.62	1.36	81.5	0.5	20
JO206	109.677	1.60	1.30	−87.4	0.7	23
JW100	108.644	2	1.7	8.3	0.9	24

and tails, mosaics have been necessary. The actual configurations used for the observations allowed us to sample scales up to the maximum recoverable scale (MRS), reported in Table 1 for each galaxy.

The data have been calibrated and imaged using the CASA software (version 5.4.0-7; McMullin 2007), as described in Moretti et al. (2020). The details of the obtained line images are reported in Table 1

From the cleaned data cubes we obtained moment-zero maps, using the SOFIA software (Serra et al. 2015) to construct detection masks for each ALMA datacube, as described in Moretti et al. (2020) for JW100. Figure 1 shows the CO(1–0) moment-zero for the disks of the four galaxies analyzed here.

For each galaxy we measure both the amount of molecular gas within the stellar disk and outside it, where the CO is located in correspondence with the ionized gas tails found in Poggianti et al. (2017b), Bellhouse et al. (2017), Gullieuszik et al. (2017), and Poggianti et al. (2019). We use here as a disk definition the one given in Gullieuszik et al. (2020) (shown as a red contour in Figure 1), which is based on the stellar isophote at 1σ above the sky background level measured on the undisturbed side of the galaxy and then symmetrized to exclude the contribution from the stripped tail.

Table 1 shows that we will base our results on the detection of molecular gas on scales between ~ 1 and ~ 20 kpc, thus neglecting the contribution from any gas diffuse on larger scales. We do not have single dish data at the CO(1–0) frequency to assess the possible flux loss, and therefore our data are, strictly speaking, lower limits. The uncertainty on the measured fluxes is of the order of 10%.

3. Results

As shown in Figure 1, the molecular gas distribution in the galaxy disk is quite consistent with the $H\alpha$ emission (colored contours) derived from MUSE data (Bellhouse et al. 2017; Gullieuszik et al. 2017; Poggianti et al. 2017b, 2019).

For each galaxy we have used the CO(1–0) emission to derive the CO flux and the H_2 mass using the following equation from Watson & Koda (2017):

$$\left(\frac{M_{H_2}}{M_\odot}\right) = 1.1 \times 10^4 \left(\frac{\alpha_{CO}}{4.3}\right) \left(\int S_{10} dv\right) (D_L)^2, \quad (1)$$

where α_{CO} is the CO-to- H_2 conversion factor expressed in $M_\odot (\text{K km s}^{-1} \text{ pc}^2)^{-1}$, S_{10} is the CO flux density in janskys and D_L is the luminosity distance in megaparsecs.

As is well known, the H_2 mass is strongly dependent on the α_{CO} factor. Table 2 gives the molecular gas masses for different assumptions on α_{CO} , as well as the SFRs measured within the

⁹ <https://web.oapd.inaf.it/gasp/>

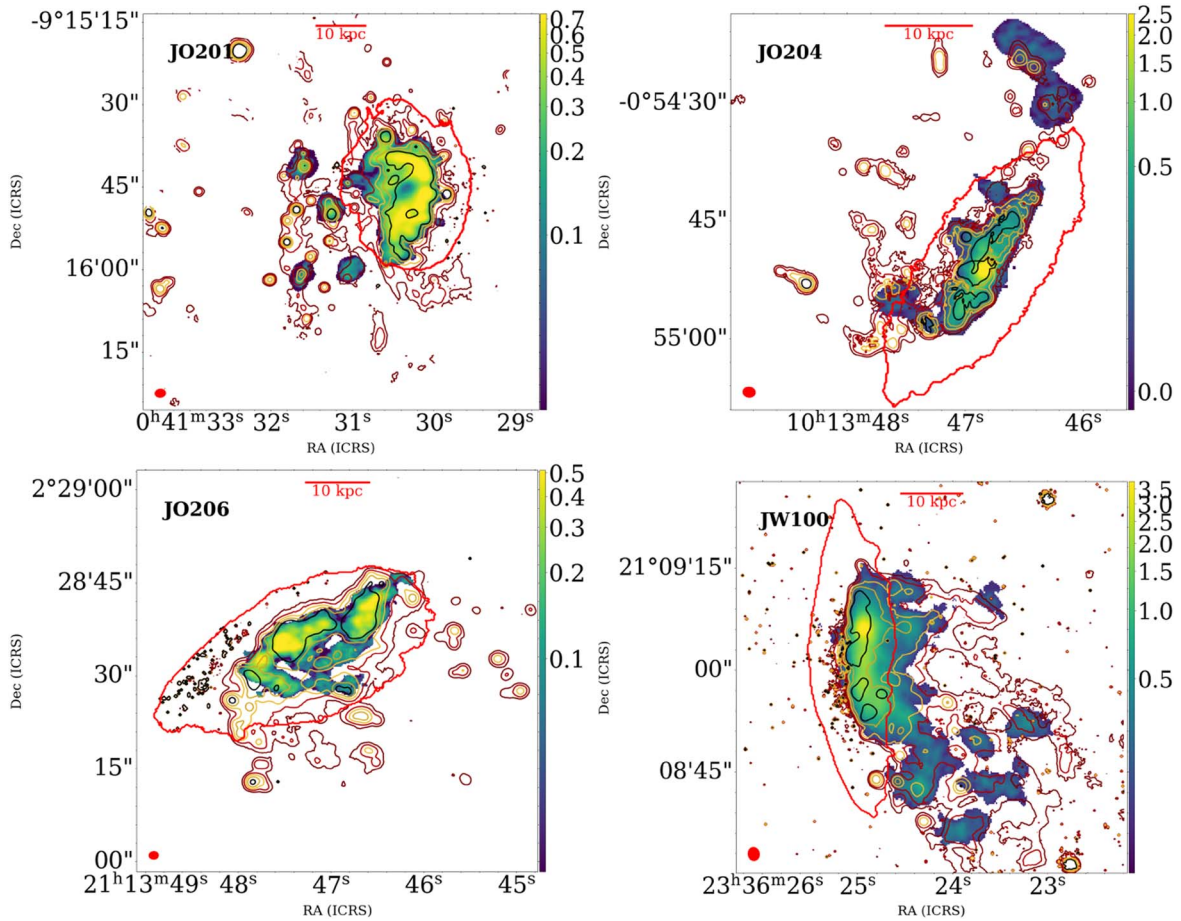


Figure 1. CO(1–0) moment-zero maps (in scale colors) in $\text{Jy beam}^{-1} \text{km s}^{-1}$ for JO201, JO204, JO206, and JW100. Colored contours show the $\text{H}\alpha$ emission derived from MUSE data at 2×10^{-17} , 4×10^{-17} , 8×10^{-17} , 1.6×10^{-16} , and $3.2 \times 10^{-15} \text{ erg/cm}^2 \text{ s}^{-1} \text{ arcsec}^{-2}$, while the red contour delimits the galaxy stellar disk derived from the MUSE data (see the text for details). The scale in kiloparsecs and the beam size are also shown in red within each panel.

disk using the star-forming spaxels from Vulcani et al. (2018) and the corresponding H_2 depletion times, defined as $M_{\text{H}_2}/\text{SFR}$.

First, we used the Milky Way α_{CO} that is equal to $4.3 M_{\odot} (\text{K km s}^{-1} \text{pc}^2)^{-1}$ (Bolatto et al. 2013), including the helium correction, which is the standard value used in the literature. We used this value to calculate the molecular gas masses and the corresponding gas fractions with respect to the galaxy stellar mass, $f_{\text{H}_2} = M_{\text{H}_2}/M_{\star}$, shown as filled symbols in Figure 2.

We used the same assumption to calculate the molecular gas mass present in the tail clumps. As described in detail in A. Moretti et al. (2020, in preparation), which deals with the extraplanar emission, the molecular gas masses in correspondence to the tail star-forming clumps ($0.4\text{--}1.7 \times 10^9 M_{\odot}$) amounts to only a small fraction of the total stellar mass (see column 5 in Table 2).

As a second step, in order for our data to be comparable with the xCOLDGASS sample, we calculated the H_2 masses assuming an α_{CO} variable with the metallicity, following the relation found for the same sample by Accurso et al. (2017), that depends both on the galaxy metallicity and on its distance from the star formation main sequence. This relation, though, only holds up to metallicities of $12 + \log(\text{O}/\text{H}) = 8.8$.

We used the $[\text{O III}]/[\text{S II}^+]$ versus $[\text{N II}]/[\text{S II}^+]$ line ratio to derive the spatially resolved gas phase metallicities (Franchetto et al. 2020) for our galaxies and derived the mean α_{CO} within the disk. As our method to estimate the gas metallicity is

different from the one used by Accurso et al. (2017) our galaxies might be skewed toward higher values. This does not bias the results, though, as we mostly use the asymptotic value from the Accurso et al. (2017) relation.

As for the distance from the main sequence of the SFR–mass relation, we assumed the average value found for jellyfish galaxies in Vulcani et al. (2018), i.e., 0.15 dex.

Both using the Milky Way α_{CO} (filled symbols in Figure 2) and the metallicity-dependent one (empty symbols), we find that the total molecular gas fractions in our jellyfish galaxies are significantly larger than the mean values found for star-forming main-sequence galaxies in the xCOLDGASS sample by Saintonge et al. (2017), shown as a reference in Figure 2. Gray dots in Figure 2 are the single data points from Saintonge et al. (2017) for galaxies within 0.4 dex from the main sequence, demonstrating indeed that our jellyfishes lie at the upper edge of the observed distribution. We note that the results obtained by Bolatto et al. (2017) on a subsample of the CALIFA galaxies observed with the CARMA interferometer are perfectly in agreement with the Saintonge relation. The Virgo cluster data by Corbelli et al. (2012), represented as black filled dots in Figure 2, having rescaled the stellar masses to correct for the different assumption in the IMF, lie below the mean field relations, which led the authors to conclude that H_2 has been stripped from the galaxies.

We notice that the ram pressure acting on the infalling galaxies could in principle unbind the already existing giant molecular clouds (GMCs) in the galaxy disk, increasing the CO/H_2 ratio. If

Table 2
Molecular and Atomic Gas Properties of the Observed Galaxies

M_* 1e9 M_\odot	SFR $M_\odot \text{ yr}^{-1}$	α_{CO}	$M_{\text{H}_2, \text{in}}$ 1e9 M_\odot	$M_{\text{H}_2, \text{out}}$	$\tau_{\text{dep}, \text{H}_2}$ Gyr	$M_{\text{H I}}$ 1e9 M_\odot	R_{mol}	M_{gas}/M_*	$\tau_{\text{dep}, \text{tot}}$ Gyr
JO201									
35.5	5 ± 1	4.3	16.5[46%]	2%	3.3	1.15	14	0.53	3.5
		3.0^a	11.5[32%]		2.3		10	0.39	2.6
		1.3^b	5.0[14%]		1		4	0.21	1.3
JO204									
40	1.5 ± 0.3	4.3	8.1[20%]	1%	5.4
		3.0^a	5.7[14%]		3.9
		1.4^b	2.7[7%]		1.8
JO206									
90	4.8 ± 0.9	4.3	8.7[10%]	0.4%	1.8	0.7	12	0.14	1.9
		2.8^a	5.6[6%]		1.2		8	0.10	1.3
		2.0^b	4.0[4%]		0.8		6	0.08	1.0
JW100									
300	2.6 ± 0.5	4.3	23.7[8%]	0.6%	9.1	0.2	132	0.09	9.2
		3.0^a	16.5[5%]		6.3		92	0.07	6.4
		0.9^b	5.0[2%]		1.9		28	0.03	2.0

Note. For each galaxy and α_{CO} assumption (a from Accurso et al. 2017 and b from Amorin et al. 2016) we list stellar masses; SFRs from H α MUSE emission within the disks from Vulcani et al. (2018); molecular gas masses within the galaxy disk assuming different α_{CO} and, in parenthesis, the molecular gas to stellar mass fractions in the disk; molecular gas to stellar mass fractions in the stripped tail; H $_2$ depletion times; H I masses within the disk from Ramatsoku et al. (2019, 2020) and T. Deb et al. (2020, in preparation); $R_{\text{mol}} = M_{\text{H}_2}/M_{\text{HI}}$ in the disks; and total gas fractions (molecular+neutral, disks+tails) and corresponding total depletion times for the different α_{CO} .

this were the case, for a correct estimate of the molecular gas mass we should be using a lower α_{CO} , more similar to that found, for example, in ULIRGs (see Bolatto et al. 2013; Sandstrom et al. 2013; Israel et al. 2015) where the underlying cold gas distribution is more diffuse. To mimic this effect, we also used a second metallicity-dependent formulation of α_{CO} (Amorin et al. 2016; which gives results compatible with the studies by Schrubba et al. 2012 and Genzel et al. 2012 for higher redshift galaxies) where this factor reaches values that go from 0.9 (in JW100) to 2.0 (in JO206). The corresponding molecular gas masses are also given in Table 2.

With these assumptions we find the molecular gas fractions, shown in Figure 2 as arrows, which are closer to the literature relations. We caution, however, that these extremely low conversion factors have been extrapolated using relations meant to include primarily low metallicity galaxies. The behavior of the α_{CO} in the high metallicity range is still debated, as some authors do not find significant deviations from the MW value (Wolfire et al. 2010; Sandstrom et al. 2013).

We conclude that the molecular gas fractions we derive for our jellyfish galaxies are much higher than in both field galaxies and in the Corbelli et al. Virgo cluster galaxies. Using a constant MW-like α_{CO} , the molecular gas fractions at given stellar mass are higher than the mean values in xCOLDGASS galaxies by an average factor of ~ 5 , while using the Accurso et al. (2017) relation by an average factor of ~ 4 , with molecular gas fractions ranging between $\sim 8\%$ and $\sim 50\%$. The derived H_2 masses are extremely high, ranging between 8 and $24 \times 10^9 M_\odot$. Using a second metallicity-dependent α_{CO} (plausible if the molecular gas were much more diffuse than usual due to the ram pressure actually disrupting GMCs, but highly uncertain at the high metallicities of our galaxies) yields molecular gas fractions closer to the literature

values for nonstripped galaxies, though still well above the mean for field galaxies and still higher than those observed in Virgo spirals. Thus, unless the α_{CO} is close to the value mostly found in ULIRGs (in the sense that most of the molecular gas is diffuse), jellyfish galaxies have huge reservoirs of H_2 .

The standard molecular depletion time in galaxy disks, resolved on an ~ 1 kpc scale, is ~ 2 Gyr (Bigiel et al. 2008; Leroy et al. 2008). The H_2 depletion timescales of our jellyfishes are significantly longer if we consider MW-like α_{CO} , except for JO206 (2). When using the Accurso et al. (2017) scaling relation, the timescales for JW100 and JO204 are still longer than normal galaxies, while the other two are more consistent with the literature values (JO201 and JO206). Assuming a very low α_{CO} over the entire extent of the disk leads to timescales generally shorter than in normal galaxies.

3.1. H_2/HI Mass Ratio, Total Gas Mass Fractions, and Depletion Times

Having established that molecular gas is abundantly present in jellyfish galaxies, we now proceed to evaluate the proportion of the different gas phases within the galaxy disk to better characterize the star-forming cycle. Three of our galaxies (Ramatsoku et al. 2019, 2020; T. Deb et al. 2020, in preparation) also possess an estimate of the H I gas content (preliminary from MeerKat data for JW100), while for the fourth one (JO204) this has been hampered by H I absorption due to the presence of a continuum source at the center of the galaxy (Deb et al. 2020). We note that within the disk the neutral and the molecular gases have similar distributions, at the observed spatial scales. For the JO206 galaxy we had to recalculate the mass within the disk using the disk definition adopted here.

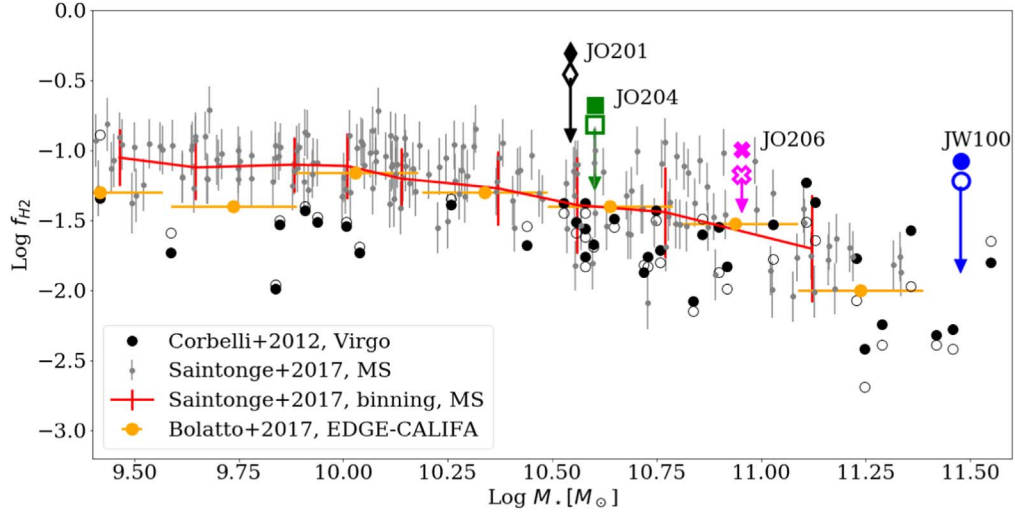


Figure 2. Total molecular gas fraction f_{H_2} ($=M_{\text{H}_2}/M_*$) as a function of the stellar mass. H_2 masses have been derived using a constant α_{CO} (filled symbols) and two different metallicity-dependent α_{CO} : the Accurso et al. (2017; empty symbols) and the Amorin et al. (2016; arrows). The red line shows the mean scaling relation found in the xCOLDGASS survey by Saintonge et al. (2017) for field galaxies on the main sequence, and gray dots are the single measurements. Orange dots refer to spiral galaxies from the EDGE-CALIFA survey (Bolatto et al. 2017). Black dots are H I deficient galaxies in Virgo from Corbelli et al. (2012): filled symbols and empty symbols represent H_2 masses derived with constant or metallicity-dependent α_{CO} .

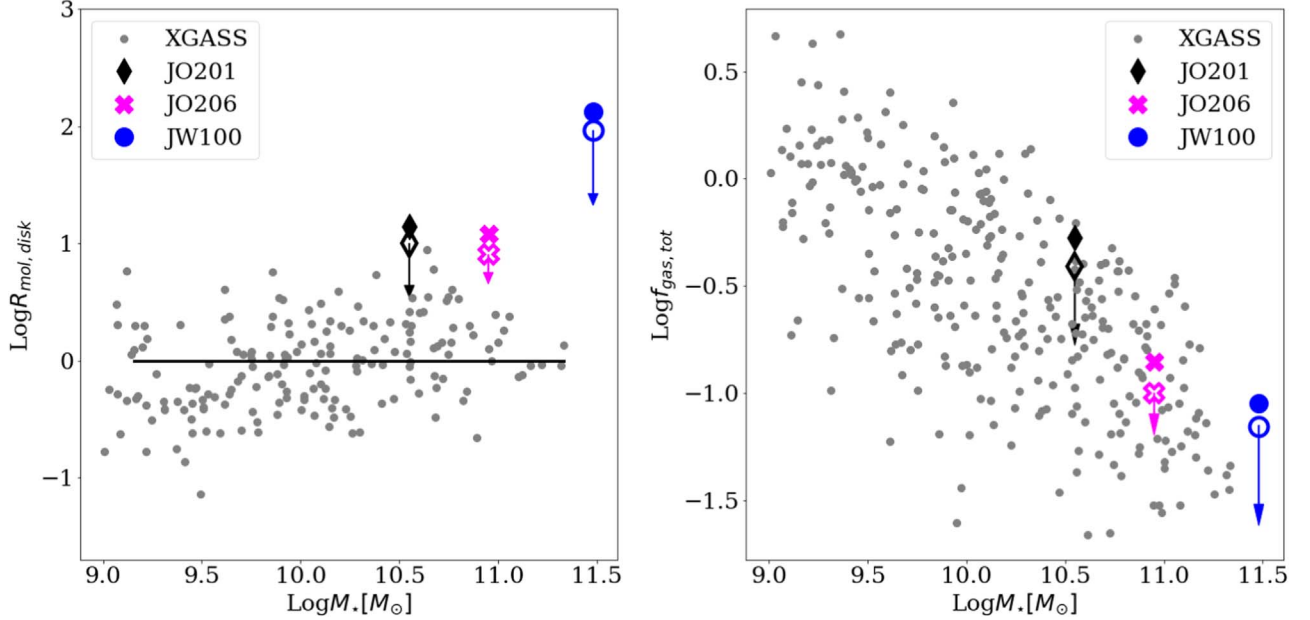


Figure 3. Molecular gas fraction ($R_{\text{mol,disk}} = M_{\text{H}_2,\text{disk}}/M_{\text{H I,disk}}$) in the disk (left) and total gas fraction ($f_{\text{gas,tot}} = (M_{\text{H}_2,\text{tot}} + M_{\text{H I,tot}})/M_*$) (right) for JO201, JO206, and JW100 compared with the XGASS sample as a function of the stellar mass from Wang et al. (2020) and Catinella et al. (2018). The black horizontal line shows the average R_{mol} of the sample.

In Figure 3 we show the disk molecular gas fraction $R_{\text{mol}} = M_{\text{H}_2}/M_{\text{H I}}$ of these three galaxies, compared with the values in spiral disks derived from the xGASS sample assuming a radial fit to the H I mass distribution (Wang et al. 2020). R_{mol} in the disk of our galaxies turns out to be very high (ranging from 4 to ~ 100), while the average expected value in galaxy disks is $R_{\text{mol}} = 1$ (black horizontal line in Figure 3). Our data are clearly significantly offset compared to normal galaxies with the same stellar mass. This result persists for any assumption on α_{CO} .

Since R_{mol} can be considered proportional to the ratio between the typical GMC lifetime over the conversion time between the neutral and the molecular phase (Leroy et al. 2008), our results strongly suggest that the conversion of H I

into molecular gas is very efficient in jellyfish galaxies. We note that similar trends have been found also in interacting galaxies (Casasola et al. 2004).

Strikingly, summing up the molecular and neutral gas masses and considering the total (disk and tail) ratio of gas and stellar masses, we obtain gas mass fractions (shown in the right panel of Figure 3) that are within the observed range of normal galaxies. In other words, the total gas (molecular+neutral) associated to our jellyfish galaxies (considering both what is left in the disk and what is in the tail) is normal for their stellar mass. These results do not change if we restrict these comparisons to normal galaxies within the range of stellar mass surface density similar to ours (that goes from 8 to $9 M_{\odot} \text{ kpc}^{-2}$).

Finally, considering depletion times, we note that in Ramatsoku et al. (2020), for JO201 and JO206, we found that HI depletion times are much shorter than the average value found in galaxy disks, apparently implying a very efficient star formation (as far as HI is concerned) and/or a low HI content for their SFR. Evaluating the global (HI + H₂) depletion time for the three galaxies where we have both measurements, it turns out that within the galaxy disk the estimated depletion time is in agreement with literature values (Leroy et al. 2008) only for the JO206 galaxy, while JO201 and JW100 have unusually long depletion times, unless we assume extremely low values for the α_{CO} .

4. Conclusions

Our analysis of the molecular gas content of four GASP ram-pressure stripped galaxies measured on 1 kpc scale with ALMA reveals a very high molecular gas fraction with respect to both isolated/field galaxies and Virgo cluster galaxies with a similar stellar mass.

Our results are dependent on the assumptions on the α_{CO} , but even assuming a very low α_{CO} (~ 1 , so far observed mostly in ULIRGs) the H₂ content is higher than typical values for normal galaxies of the same mass.

When considering the neutral gas still present in the disk, we find an enhanced molecular-to-neutral gas ratio R_{mol} with respect to undisturbed galaxies (Wang et al. 2020; even when using the lowest α_{CO}), and at the same time a total gas fraction, which is in good agreement with the scaling relations for normal spirals found by Catinella et al. (2018).

These results strongly suggest that the gas compression caused by the ram pressure in the peak stripping phase causes the conversion of large amounts of HI into the molecular phase in the disk, possibly implying that only part of the HI gets efficiently stripped.











We acknowledge funding from the agreement ASI-INAF n.2017-14-H.0, as well as from the INAF main-stream funding program. B.V., M.G., and R.P. also acknowledge the Italian PRIN-Miur 2017 (PI A. Cimatti). This project has received funding from the European Research Council (ERC) under the European Union's Horizon 2020 research and innovation program (grant agreement No. 833824, GASP project and grant agreement No. 679627, FORNAX project). We acknowledge S. Tonnesen and Y. Jaffé for the stimulating discussion and J. Wang for sharing in electronic format her data. This paper makes use of the following ALMA data: ADS/JAO.ALMA#2017.1.00496.S. ALMA is a partnership of ESO (representing its member states), NSF (USA) and NINS (Japan), together with NRC (Canada) and NSC and ASIAA (Taiwan), in cooperation with the Republic of Chile. The Joint ALMA Observatory is operated by ESO, AUI/NRAO and NAOJ. Based on observations collected by the European Organisation for Astronomical Research in the Southern Hemisphere under ESO program 196.B-0578 (VLT/MUSE). This research made use of APLpy, an open-source plotting package for Python (Robitaille and Bressert, 2012; Robitaille, 2019).

Facilities: ALMA, VLT(MUSE).

Software: CASA (McMullin & Waters 2007).

ORCID iDs

Alessia Moretti  <https://orcid.org/0000-0002-1688-482X>
Rosita Paladino  <https://orcid.org/0000-0001-9143-6026>
Bianca M. Poggianti  <https://orcid.org/0000-0001-8751-8360>

Paolo Serra  <https://orcid.org/0000-0001-5965-252X>
Mpati Ramatsoku  <https://orcid.org/0000-0003-0231-3249>
Andrea Franchetto  <https://orcid.org/0000-0001-9575-331X>
Marco Gullieuszik  <https://orcid.org/0000-0002-7296-9780>
Neven Tomičić  <https://orcid.org/0000-0002-8238-9210>
Matilde Mingozzi  <https://orcid.org/0000-0003-2589-762X>
Benedetta Vulcani  <https://orcid.org/0000-0003-0980-1499>
Mario Radovich  <https://orcid.org/0000-0002-3585-866X>
Daniela Bettoni  <https://orcid.org/0000-0002-4158-6496>
Jacopo Fritz  <https://orcid.org/0000-0002-7042-1965>

References

- Accurso, G., Saintonge, A., Catinella, B., et al. 2017, *MNRAS*, 470, 4750
Amorín, R., Muñoz-Tuñón, C., Aguerrí, J. A. L., & Planesas, P. 2016, *A&A*, 588, A23
Bellhouse, C., Jaffé, Y. L., Hau, G. K. T., et al. 2017, *ApJ*, 844, 49
Bigiel, F., Leroy, A., Walter, F., et al. 2008, *AJ*, 136, 2846
Bigiel, F., Leroy, A. K., Walter, F., et al. 2011, *ApJL*, 730, L13
Bigiel, F., Walter, F., Blitz, L., et al. 2010, *AJ*, 140, 1194
Bolatto, A. D., Wolfire, M., & Leroy, A. K. 2013, *ARA&A*, 51, 207
Bolatto, A. D., Wong, T., Utomo, D., et al. 2017, *ApJ*, 846, 159
Boselli, A., Cortese, L., Boquien, M., et al. 2014, *A&A*, 564, A67
Boselli, A., Gavazzi, G., Lequeux, J., et al. 1997, *A&A*, 327, 522
Casasola, V., Bettoni, D., & Galletta, G. 2004, *A&A*, 422, 941
Casasola, V., Bianchi, S., De Vis, P., et al. 2020, *A&A*, 633, A100
Catinella, B., Saintonge, A., Janowiecki, S., et al. 2018, *MNRAS*, 476, 875
Chabrier, G. 2003, *PASP*, 115, 763
Corbelli, E., Bianchi, S., Cortese, L., et al. 2012, *A&A*, 542, A32
Cortese, L., Catinella, B., Boissier, S., Boselli, A., & Heinis, S. 2011, *MNRAS*, 415, 1797
Cortese, L., Catinella, B., & Janowiecki, S. 2017, *ApJL*, 848, L7
Deb, T., Verheijen, M. A. W., Gullieuszik, M., et al. 2020, *MNRAS*, 494, 5029
Fernández, X., Gim, H. B., Gorkom, J. H. v., et al. 2016, *ApJL*, 824, L1
Franchetto, A., Vulcani, B., Poggianti, B. M., et al. 2020, *ApJ*, 895, 106
Genzel, R., Tacconi, L. J., Combes, F., et al. 2012, *ApJ*, 746, 69
George, K., Poggianti, B. M., Gullieuszik, M., et al. 2018, *MNRAS*, 479, 4126
Gullieuszik, M., Poggianti, B. M., McGee, S. L., et al. 2020, *ApJ*, in press (arXiv:2006.16032)
Gullieuszik, M., Poggianti, B. M., Moretti, A., et al. 2017, *ApJ*, 846, 27
Israel, F. P., Rosenberg, M. J. F., & van der Werf, P. 2015, *A&A*, 578, A95
Jáchym, P., Combes, F., Cortese, L., Sun, M., & Kenney, J. D. P. 2014, *ApJ*, 792, 11
Jáchym, P., Kenney, J. D. P., Sun, M., et al. 2019, *ApJ*, 883, 145
Jáchym, P., Sun, M., Kenney, J. D. P., et al. 2017, *ApJ*, 839, 15
Kenney, J. D. P., & Young, J. S. 1989, *ApJ*, 344, 171
Kennicutt, R. C. 1998, *ARA&A*, 36, 189
Leroy, A. K., Walter, F., Brinks, E., et al. 2008, *AJ*, 136, 2782
Leroy, A. K., Walter, F., Sandstrom, K., et al. 2013, *AJ*, 146, 19
McMullin, J. P., & Waters, B. S. D. Y. W. G. K. 2007, in ASP Conf. Ser., *Astronomical Data Analysis Software and Systems XVI*, ed. F. H. R. A. Shaw & D. J. Bell (San Francisco, CA: ASP), 127
Moretti, A., Paladino, R., Poggianti, B. M., et al. 2018, *MNRAS*, 480, 2508
Moretti, A., Paladino, R., Poggianti, B. M., et al. 2020, *ApJ*, 889, 9
Poggianti, B. M., Ignesti, A., Gitti, M., et al. 2019, *A&A*, 887, 155
Poggianti, B. M., Jaffé, Y. L., Moretti, A., et al. 2017a, *Natur*, 548, 304
Poggianti, B. M., Moretti, A., Gullieuszik, M., et al. 2017b, *ApJ*, 844, 48
Ramatsoku, M., Serra, P., Poggianti, B. M., et al. 2019, *MNRAS*, 487, 4580
Ramatsoku, M. A., Serra, P., Poggianti, B. M., et al. 2020, *A&A*, in press (arXiv:2006.11543)
Saintonge, A., Catinella, B., Tacconi, L. J., et al. 2017, *ApJS*, 233, 22
Saintonge, A., Kauffmann, G., Kramer, C., et al. 2011a, *MNRAS*, 415, 32
Saintonge, A., Kauffmann, G., Wang, J., et al. 2011b, *MNRAS*, 415, 61
Sandstrom, K. M., Leroy, A. K., Walter, F., et al. 2013, *ApJ*, 777, 5
Schmidt, M. 1959, *ApJ*, 129, 243
Schrubba, A., Leroy, A. K., Walter, F., et al. 2012, *AJ*, 143, 138
Serra, P., Westmeier, T., Giese, N., et al. 2015, *MNRAS*, 448, 1922
Vulcani, B., Poggianti, B. M., Gullieuszik, M., et al. 2018, *ApJL*, 866, L25
Wang, J., Catinella, B., Saintonge, A., et al. 2020, *ApJ*, 890, 63
Watson, L. C., & Koda, J. 2017, in *Outskirts of Galaxies, Astrophysics and Space Science Library*, Vol. 434, ed. L. J. C. Galaxies, J. H. Knapen, & A. G. de Paz (Berlin: Springer), 175
Wolfire, M. G., Hollenbach, D., & McKee, C. F. 2010, *ApJ*, 716, 1191